2023 IEEE International Conference on Acoustics, Speech, and Signal Processing Workshops (ICASSPW) | 979-8-3503-0261-5/23/$31.00 ©2023 IEEE | DOI: 10.1109/ICASSPW59220.2023.10193476

ON THE COMPLEXITY OF NON-COHERENT ACQUISITION OF CHIRP SPREAD SPECTRUM SIGNALS

Daniel Egea-Roca, José A. López-Salcedo, Gonzalo Seco-Granados

Dpt. of Telecommunications and Systems Engineering, IEEC-CERES, UAB, Spain

ABSTRACT

During the past few decades, the use of GNSSs has become the primary and sometimes only way of providing a positioning solution for many outdoor applications. Furthermore, GNSS is playing an important role on the development of smart cities and Internet of things (IoT) applications. Unfortunately, GNSS is a technology that is a very hungry technology thus challenging its adoption in many IoT application. All these ingredients boil down to the need for alternative positioning solutions to backup GNSS. The use of low-Earth orbit (LEO) satellite constellations has been considered in the literature for that purpose. Chirp Spread Spectrum (CSS) modulation is a different approach to classic GNSS to enable positioning with LEO satellites. This type of signal is intended to address low-complexity positioning for IoT devices, tackling the complexity issue of the classic GNSS acquisition. In this paper, we consider the analysis of the non-coherent acquisition of CSS signals and its complexity is compared to its coherent counterpart.

***Index Terms*—** CSS, GNSS, LEO, low-complexity, non-coherent acquisition

1. INTRODUCTION

Thanks to the technology development of low-power wide-area network (LPWAN) and the excellent positioning capabilities provided by global navigation satellite systems' (GNSSs), the application of the Internet of Things (IoT) has reached every corner of human activity [1]. As a consequence, the stringent requirements of the wide-range of applications in the IoT sector has pushed the capabilities of both LPWAN and GNSS to their limits. This has placed several lines of development to boost the performance of these sectors. For instance, the coverage limitation of terrestrial IoT communication networks is planned to be solved with the use of low-Earth orbit (LEO) satellite constellations [2]. In the GNSS side, we should note the extremely high power consumption of current receiver devices. Thus failing on providing the low-power consumption required for IoT devices [3]. In the past few years, several evolutionary paths of GNSS have been launched to solve this problem [4].

The complementary of GNSS with telecom. systems is one of the aspects getting more importance in the last decade. Furthermore, it will become crucial in the coming years thanks to the novel list of LEO satellite constellations for broadband internet services or IoT connectivity [5, 6]. The opportunities of LEO constellations have shown to deal with the main challenges of IoT communication and localization systems, bringing some advantages wrt to medium-Earth orbit (MEO) constellations [7]: frequency diversity, improvement on geometry of dilution, and they experience less propagation losses. Based on these considerations, the scientific and commercial interest on LEO-based positioning, navigation and timing (PNT) for GNSS complementary has been triggered during the last years [8].

1.1. Related Literature

The first PNT results from the Starlink constellation were published in Fall 2021 [9]. This opened a new era of alternative PNT solutions based on signals of opportunity (SoO) from LEO constellations or by the development of an alternative LEO PNT system [10]. One of the most important tasks of such a system is to design the signal to be transmitted from the satellites. Different options can be adopted for the signal design, but if we aim to reduce complexity wrt current GNSS we should change the current signal structure [7, 8]. Otherwise, the signal acquisition would be prohibitive for IoT devices. The signal acquisition is needed to identify the satellites in view and to get a coarse estimation of their range to the user. This is a fundamental information for the computation of the PNT solution.

Note the high dynamic in LEO constellations will produce a large search space for the acquisition process of a GNSS signal [7]. One alternative with lower acquisition complexity in LEO can be based on a chirp spread spectrum (CSS) signal. Improvements in terms of complexity from 1 up to 2 orders of magnitude can be obtained [7]. Furthermore, [8] provides details on the key performance indices (KPI) for PNT of the CSS signal. In particular, [7] and [8] consider for the first time the use of a CSS signal for PNT and evaluate its performance for the signal design in a LEO constellation. The goal was to consider the migration in the terrestrial and LEO satellite domain from DSSS signaling (with high-end receivers) to CSS signaling for low-power (and low-complexity) communications and positioning, but for the case of positioning with LEO satellites.

1.2. Contribution

Motivated by the simplicity of the CSS signal processing, in this paper we aim at extending the knowledge adquired in [7] and [8] on the complexity of the CSS signal for LEO-PNT. One common practice in GNSS technology for low-power consumption is the application of non-coherent integration (NCI) techniques for the acquisition of the GNSS signal [4]. These techniques allow the receiver to acquire the GNSS signals with small pieces of signal, thus reducing the time the receiver is active. Traditionally, NCI techniques are used to improve the sensitivity performance of the receivers for a given integration time. In this paper, though, the focus is to evaluate the effects of a NCI into the signal processing complexity.

Specifically, the contribution of this paper is twofold: (i) we provide a concise and simple description of the signal design, receiver processing and performance analysis of a CSS signal for LEO-PNT; and (ii) we analyze the perfomrance of a non-coherent acquisition

This work was partly supported by the Spanish Ministry of Science and Innovation under Grant PID2020-118984GB-I00 and by the European Space Agency (ESA) under the INNUENDO project (ESA ITT AO/1-9585/19/NL/CRS).

of the CSS signal proposed for LEO-PNT. The effects on the sensitivity performance and more importantly on the receiver processing complexity are analyzed. The results are compared with a classical coherent acquisition of the CSS signal. To do so, we first provide in Section 2 the signal model used throughout the paper. Second, Section 3 provides the performance analysis framework considered in this paper. Then, Section 4 provides the numerical results and Section 5 concludes this paper.

2. SIGNAL MODEL

In this section we introduce the main parameters and concepts useful to undestand the analysis of the CSS signal carried out in this paper. More specifically, we first describe the signal structure of the CSS signal used in this paper. Note this signal structure was already proposed in [7]. Then, we introduce the low-complexity process used to coherently acquire the CSS signal, already used in [8]. Finally, we define the novel non-coherent acquisition analyzed in this paper.

2.1. CSS Signal Structure

A CSS signal is a frequency-varying signal that changes its frequency in a given bandwidth B during the chirp duration (or period) $T_{\rm c}$. Linear chirps are extensively used in practice and they are completely characterized by the chirp rate (or slope) [1]: $\mu \doteq B/T_{\rm c}$. In a satellite propagation channel, and particularly for LEO constellations, we have to consider the presence of both time-delay, τ, and frequency Doppler, $f_{\rm D}$. In such a case, as explained in [7], we need the transmission of two chirp components: one with positive and another with negative slope; the so-called BOK-chirp signal.

Furthermore, for a PNT system we need the transmission of different signals from the different satellites in the constellation [11]. So, the following signal model is considered for the received signal:

$$r(t) = \sum_{i=1}^{N_{\rm vis}} s_i(t-\tau_i) e^{j2\pi f_{\rm D}^{(i)}(t-\tau_i)} + \omega(t), \tag{1}$$

where $N_{\rm vis}$ is the number of visible satellites, $s_i(t)$, with $i = 1, 2, \ldots, N_{\rm vis}$, is the transmited BOK-chirp signal, $\{\tau_i, f_{\rm D}^{(i)}\}$ denote the time-delay and Doppler frequency of the i-th satellite, respectively, and $w(t)$ is the AWGN. For the generation of the different signal waveforms we consider the multi-dual slope (MDS) scheme proposed in [7] and analyzed in [8].

For a constellation with $N_{\rm sat}$ satellites, this scheme assign two different chirp rates for every satellite in the following way:

$$\mu_i^{(1)} = i\frac{2\mu}{N_{\rm sat}} \quad \text{and} \quad \mu_i^{(2)} = 2\mu - \mu_i^{(1)}, \tag{2}$$

with $i = 1, 2, \ldots, N_{\rm sat}$. Then, the transmitted signal for the i-th satellite is writen as

$$s_i(t) = \begin{cases} A\cos\left(\phi_i^{(1)}(t)\right), & t \le \frac{T_{\rm c}}{2} \\ A\cos\left(\theta_0 + \phi_i^{(2)}(t)\right), & \frac{T_{\rm c}}{2} < t \le T_{\rm c} \end{cases}, \tag{3}$$

with $\theta_0 = \pi(\mu_i^{(2)} - \mu_i^{(1)})T_{\rm c}/2$, $A = \sqrt{2P_{\rm s}}$, $P_{\rm s}$ the received signal power, and

$$\phi_i^{(j)}(t) = 2\pi \int_0^t \left[\mu_i^{(j)} u\right]_B {\rm d}u \tag{4}$$

where $j = 1, 2$, and $[x]_B$ stands for the modulus B operator of x.

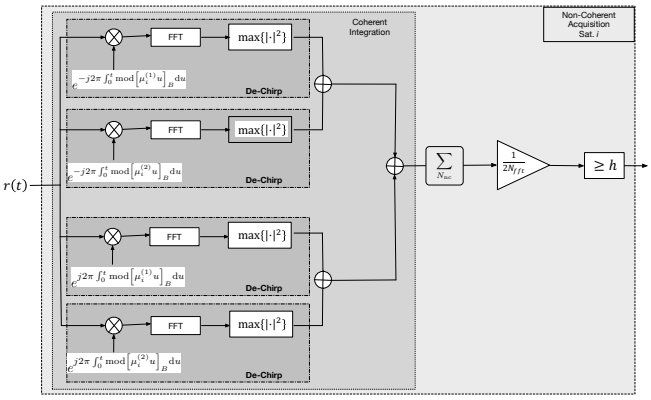

Fig. 1. Non-Coherent acquisition block for one satellite.

2.2. Coherent Acquisition

To understand the coherent acquisition of the MDS signal of a given satellite it is worth studying the traditional way of processing a CSS signal in a simple fashion, namely the de-chirp process. To do so, let us first note that the BOK-chirp signal can be writen as the combination of two (i.e., $\pm$) chirp components $s_\pm(t) = e^{\pm j2\pi \int_0^t [\mu t]_B {\rm d}u}$. When received, each chirp component is processed by the so-called de-chirp process highlighted in Fig. 1. It consist on a local replica multiplacion followed by a fast Fourier transform (FFT) computation plus getting its maximum (squared absolute value). The coherent acquisition process of the MDS signal in (3) is also indicated in Fig. 1, and it consists of a total of 4 de-chirp processes that are added together [8]. The result is compared with a threshold to declare the presence or absence of the satellite for which the de-chirp is performed. More details on the design and performance of the coherent acquisition block will be provided in Section 3.

2.3. Non-Coherent Acquisition

The previous coherent acquisition process assumes an integration time equal to the chirp period $T_{\rm c}$. That is, the de-chirp process is performed with a piece of signal of length $T_{\rm c}$. In this paper, we consider the extension of such integration time considering the acquisition process in Fig. 1. The same architecture as in [8] is considered, but we extend the integration time by accumulating $N_{\rm nc}$ outputs of the coherent acquisition. In other words, we define the total integration time as $T_{\rm int} \doteq N_{\rm nc} T_{\rm coh}$ and the following test statistic is used for acquisition of the i-th satellite at the k-th NCI interval:

$$\mathcal{T}_{\rm nc}^{(i)}(k) = \sum_{l=(k-1)+1}^{N_{\rm nc}k} \mathcal{T}_l^{(i)}, \tag{5}$$

where $\mathcal{T}_l$ denotes the coherent integration output at the l-th coherent integration interval.

3. NCI: PERFORMANCE ANALYSIS

This section defines the KPI useful to analyze the performance and signal design of the MDS signal when considering an NCI scheme. It is worth noticing that this analysis and signal design target the minimization of the receiver complexity, as done in [8]. To achieve this goal we aim at minimizing the chirp period, but at the same time we sought for a large enough chirp period to satisfy different

requirements (e.g., sensitivity or accuracy). With this setting, the ultimate chirp period design is driven by the main outcomes of the performance assessment of the MDS signal [8]. In this section, we deal with the comparison of the complexity of a NCI scheme and a *full* coherent integration scheme. Specifically, we focus our analysis on the two following KPIs: the *sensitivity performance* and the *signal prcessing complexity*. Next, we define and explain the process to analyze these KPIs for an NCI scheme and how to compare them with a coherent integration scheme. The numerical results of such analysis will be provided in Section 4.

3.1. Sensitivity Performance

The value of the detection threshold used in the acquisition module of the MDS receiver shown in Fig. 1 is configured to provide certain acquisition performance for each satellite. This performance is characterized by the probabilities of false alarm (PFA) and detection (PD) of the acquisition module, respectively defined as

$$\begin{aligned} P_{\rm fa}(h) &\doteq \Pr\left\{\mathcal{T}_{\rm nc} \geq h|\mathcal{H}_0\right\} = 1 - F_{\mathcal{T}_{\rm nc},0}(h), \\ P_{\rm d}(h) &\doteq \Pr\left\{\mathcal{T}_{\rm nc} \geq h|\mathcal{H}_1\right\} = 1 - F_{\mathcal{T}_{\rm nc},1}(h), \end{aligned} \tag{6}$$

with $\mathcal{H}_0$ and $\mathcal{H}_1$ the hypotheses that the signal of the i-th satellite is absent or present, respectively. In addition, $F_{\mathcal{T}_{\rm nc},j}(h)$ with $j = 0, 1$ denotes the cummulative distribution function (cdf) of the test statistics $\mathcal{T}_{\rm nc}$ under $\mathcal{H}_j$ evaluated at h.

In this paper, the detection threshold is fixed as

$$h = F^{-1}_{\mathcal{T}_{\rm nc},0}(1-\alpha), \tag{7}$$

with $\alpha = 10^{-5}$ and we would like to have $P_{\rm d}(h) = 1 - F_{\mathcal{T}_{\rm nc},1} \geq 0.9$. Of course, the sensitivity performance is dependent on the signal parameters (i.e., $T_{\rm int}$ and B) as well as system parameters such as the carrier-to-noise density ratio (CN0), $N_{\rm sat}$ and $N_{\rm vis}$. As done in [8], for the sensitivity analysis to be carried out in this paper we obtain the value of the detection threshold in (7) numerically. This threshold is then used to get the PD we obtain when $P_{\rm fa}(h) = \alpha$. The PD is also numerically computed from (6) with the generation of 10^4 Monte-Carlo realizations of the acquisition process using the previously computed threshold.

With this framework, in this paper we analyze the minimum $T_{\rm int}$ needed to obtain the target sensitivity performance when considering a given coherent time $T_{\rm coh}$. In other words, given a $T_{\rm coh}$ we find the minimum number of NCIs, $N_{\rm nc}$, needed to get the target sensitivity performance. To do so, we follow the same iterative process used in [8]: once the PD is computed for a given setting, if PD<0.9, we increase $N_{\rm nc}$ for a given $T_{\rm coh}$. If PD>0.95, we decrease $N_{\rm nc}$ for a given $T_{\rm coh}$. In both cases, re-compute the detection threshold and PD. Otherwise, we end the iterative process and define the minimum integration time as the last evaluated $T_{\rm int} = N_{\rm nc}T_{\rm coh}$ (i.e., in the last iteration giving $0.9 <$PD< 0.95).

3.2. Complexity Performance

We follow the same approach as in [8] to analyze the complexity of the non-coherent acquisition of the MDS signal. Recall from Fig. 1 that the acquisition is composed of 4 de-chirp processes, each of them based on a FFT of the product of the received signal with the local replica. Each FFT is based on a signal of $\tilde{N} = BT_{\rm coh}$ samples. Nevertheless, for a more effective FFT computation we will choose the next power of 2 of $\tilde{N}$, given by N. This gives the following formula for the computation of the complexity of a coherent acquisition: $\mathcal{C} \doteq 4N\log_2(N)$. For a non-coherent scheme we have

$$\mathcal{C}_{\rm nc} \doteq 4N_{\rm nc}N\log_2(N). \tag{8}$$

We will base on this formula to analyze the number of operations (i.e., complex additions followed by a multiplication) needed to acquire the MDS signal in a non-coherent scheme. We also want to highlight that this is the complexity needed to acquire 1 satellite with the MDS slope. The same operations have to be repeated for each satellite in the constellation.

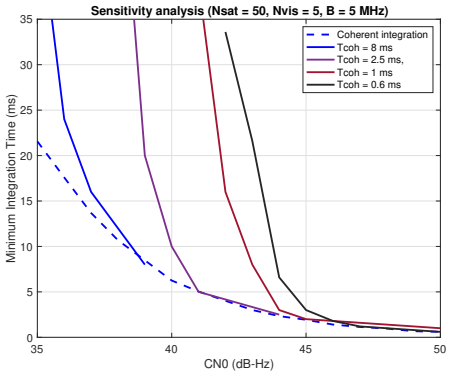

Fig. 2. Minimum integration time needed to achieve sensitivity performance as a function of the CN0.

4. NUMERICAL RESULTS

This section reports analysis of the considered NCI acquisition for the MDS signal. So, in the following we analyze the different KPIs considered in this paper, bringing light to the complexity comparison between coherent and non-coherent acquisition schemes. We will consider the following parameters for all the simulations carried out in this section: $B = 5$ MHz, $N_{\rm sat} = 50$ and $N_{\rm vis} = 5$ satellites. Furthermore, we also include the results of the coherent acquisition for all the simulations to compare them with the NCI acquisition.

4.1. Sensitivity Analysis

The results of the optimization process process described in Section 3.1 is shown in Fig. 2 for different values of $T_{\rm coh}$. The first observation we get is that the total integration time when using NCI is in general larger than the minimum chirp period needed to obtain the target sensitivity performance when integrating coherently. There are some values of $T_{\rm coh}$ that may be useful for some values of CN0. That means, that there are some values of $T_{\rm coh}$ that provides similar sensitivity performance or slightly worse than the coherent scheme. For instance, a $T_{\rm coh} \leq 2.5$ ms may be useful because in the CN0 $= [45, 50]$ dB-Hz range we get similar performance as with a coherent scheme. Based on these results, we see that a non-coherent acquisition is interesting when only performing a few NCI for a given $T_{\rm coh}$. For large NCI, it is more effective to extend the chirp period coherently. This will be confirmed next.

4.2. Complexity Analysis

Let us now analyze in detail the complexity of a non-coherent scheme for different values of the integration time. This analysis is given in Fig. 3. In general, we obtain smaller complexity values

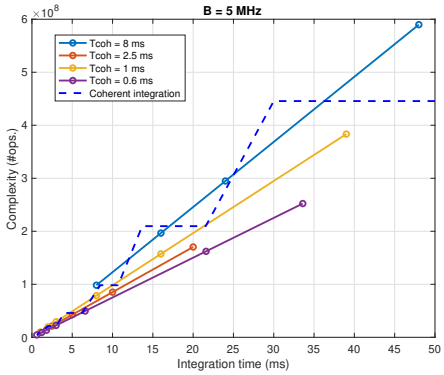

Fig. 3. Complexity as a function of the integration time.

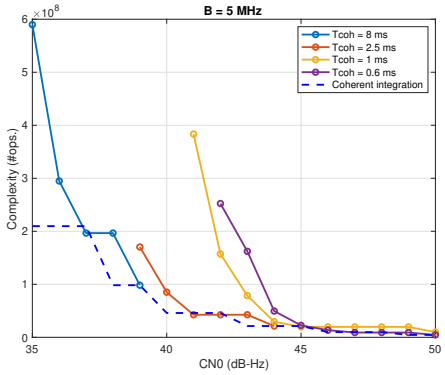

Fig. 4. Complexity as a function of the CN0 (link with sensitivity).

when using a non-coherent scheme. This is particularly true for $T_{\text{coh}} < 8$ ms. Note, there are cases in which the complexity of a non-coherent scheme becomes larger than a coherent one. For example, this is the case of $T_{\text{coh}} = 8$ ms and $T_{\text{int}} > 15$ ms. It is important to note that the complexity we obtain with the coherent and non-coherent schemes for the same integration time is on the same order of magnitude, so we will not experience a valuable difference on the complexity of both schemes using the same integration time.

4.3. Complexity Linked with Sensitivity

Let us focus in this section on the analysis of the complexity as a function of the CN0. This will allow us to extract more precise and practical conclusions. The reason is that in practice the signal will be designed to work in a given range of CN0 values. For instance, we would like to fix the integration time as the minimum value needed to obtain the target sensitivity performance at a given CN0 value. Then, the complexity should be computed from (8) but using the obtained integration time given by the sensitivity analysis. This analysis is of paramount importance, because from the previous results we see that it is possible to reduce the complexity of the coherent scheme for some values of T_{coh}. Unfortunately, with a non-coherent scheme and the same integration time in a coherent scheme, we may not obtain the target sensitivity performance for the same CN0 value. To make this clear it is useful to recall the results of Fig. 2. For instance, for $T_{\text{coh}} = 0.6$ ms and 20 ms of integration time, we are able to get target sensitivity performance @CN0 = 43 dB-Hz, but with a coherent scheme with the same integration time we obtain target sensitivity performance @ CN0 = 36 dB-Hz.

Based on the previous consideration, Fig. 4 compares the complexity of the coherent and no-coherent schemes as a function of the CN0 value used to obtain the target sensitivity performance. In general, we see how for a given CN0 value the coherent scheme provides the best results in terms of complexity for all the simulated T_{coh} values. More specifically, we see the complexity of both schemes are on the same order of magnitude for some CN0 values. However, the complexity of the non-coherent scheme is triggered wrt the one of the coherent scheme when the CN0 value is reduced. For instance, $T_{\text{coh}} = 8$ ms provides similar complexity as the coherent scheme up to 37 dB-Hz. For smaller CN0 values the non-coherent scheme is more complex than the coherent one. These results are very interesting because they show how the non-coherent acquisition is not the best suited option in terms of complexity when designing the signal to achieve the sensitivity performance requirements.

5. CONCLUSIONS

This paper has provided the basic elements to understand the signal design, processing and performance analysis of a CSS-based LEO-PNT system. As a novelty, we have provided a non-coherent scheme useful to increase the receiver sensitivity for a given signal design length or to reduce the complexity for a given integration time (wrt a coherent acquisition scheme). We have analyzed the sensitivity performance of such a scheme showing similar integration times as for a coherent scheme for high CN0 values. However, for smaller CN0 values, the integration time needed to get sensitivity performance of the non-coherent scheme is triggered wrt the integration time needed with a coherent scheme. These results are interesting because they make us think on the possibility to reduce the complexity of the CSS acquisition when using a non-coherent scheme. This is confirmed with the analysis of the complexity of the non-coherent scheme as a function of the integration time.

So, as a general conclusion of the complexity analysis of the non-coherent scheme, we can say that it may be useful (in terms of complexity at a given integration time) in a HIGH CN0 regime (i.e., 45-50 dB-Hz). Unfortunately, we must note that with a non-coherent scheme and the same integration time we may not obtain the target sensitivity performance for the same CN0 value. It is for this reason that we have compared the complexity of the coherent and no-coherent schemes as a function of the CN0 value used to obtain the target sensitivity performance. In general, the complexity of a non-coherent scheme is larger than for a coherent one at a given CN0 value. There are some CN0 values for some particular T_{coh} values that provides similar or slightly smaller complexity than a coherent scheme. It is important to note that for the same CN0 value, the complexity of both coherent and non-coherent schemes are on the same order of magnitude. For this reason, when targeting complexity optimization for a given CN0 value, it is recommend the use a coherent scheme.

As a final conclusion of the study carried out in this paper, for the sake of complexity savings we would not recommend designing the chirp period of a CSS signal according to the behavior of the non-coherent scheme. We would rely on a classical coherent scheme. That is, we recommend designing the chirp period according to the time ambiguity or the target CN0 to achieve sensitivity, depending on the use case. Then, if more sensitivity is desired, the designed chirp period could be non-coherently extended in order to acquire the signal with a smaller CN0 than the designed one.

6. REFERENCES

[1] Hai Wang and Abraham O. Fapojuwo, "A Survey of Enabling Technologies of Low Power and Long Range Machine-to-Machine Communications," *IEEE Communications Surveys and Tutorials*, vol. 19, no. 4, pp. 2621–2639, oct 2017.

[2] Chao Yang, Mei Wang, Lin Zheng, and Guangpeng Zhou, "Folded chirp-rate shift keying modulation for LEO satellite IoT," *IEEE Access*, vol. 7, pp. 99451–99461, 2019.

[3] Vicente Lucas-Sabola, Gonzalo Seco-Granados, José López-Salcedo, and José García-Molina, "GNSS IoT positioning: From conventional sensors to a cloud-based solution," *Inside GNSS*, vol. 3, no. May/June, pp. 53–62, 2018.

[4] Daniel Egea-Roca, Markel Arizabaleta-Diez, Thomas Pany, Felix Antreich, Jose A. Lopez-Salcedo, Matteo Paonni, and Gonzalo Seco-Granados, "GNSS User Technology: State-of-the-Art and Future Trends," *IEEE Access*, vol. 10, pp. 39939–39968, 2022.

[5] D. Lawrence, H. S. Cobb, G. Gutt, M. O'Connor, T. G. R. Reid, T. Walter, and D. Whelan, "Navigation from LEO: Current capability and future promise," *GPS World*, jun 2017.

[6] Tyler G.R. Reid, Andrew M. Neish, Todd Walter, and Per K. Enge, "Broadband LEO Constellations for Navigation," *NAVIGATION: Journal of the Institute of Navigation*, vol. 65, no. 2, pp. 205–220, jun 2018.

[7] Daniel Egea-Roca, José A. López-Salcedo, Gonzalo Seco-Granados, and Emanuela Falletti, "Comparison of Several Signal Designs Based on Chirp Spread Spectrum (CSS) Modulation for a LEO PNT System," in *Proceedings of the 34th International Technical Meeting of the Satellite Division of the Institute of Navigation (ION GNSS+)*. sep 2021, pp. 2804–2818, Institute of Navigation.

[8] Daniel Egea-Roca, Jose Lopez-Salcedo, Gonzalo Seco-Granados, and Emanuela Falletti, "Performance Analysis of a Multi-Slope Chirp Spread Spectrum Signal for PNT in a LEO Constellation," in *10th Workshop on Satellite Navigation Technology (NAVITEC)*. 2022, Institute of Electrical and Electronics Engineers Inc.

[9] Mohammad Neinavaie, Joe Khalife, and Zaher M. Kassas, "Exploiting Starlink Signals for Navigation: First Results," in *Proceedings of the 34th International Technical Meeting of the Satellite Division of the Institute of Navigation, ION GNSS+*. sep 2021, pp. 2766–2773, Institute of Navigation.

[10] Tyler G.R. Reid, Bryan Chan, Ashish Goel, Kazuma Gunning, Brian Manning, Jerami Martin, Andrew Neish, Adrien Perkins, and Paul Tarantino, "Satellite Navigation for the Age of Autonomy," in *IEEE/ION Position, Location and Navigation Symposium, PLANS*. apr 2020, pp. 342–352, Institute of Electrical and Electronics Engineers Inc.

[11] Peter J G Teunissen and Oliver Montenbruck, *Handbook of Global Navigation Satellite Systems*, vol. 10, Springer, 2017.